Mech. Adv. Technol., Vol. 10, No. 1, 2026, pp. 36–43

DOI: 10.20535/2521-1943.2026.10.1(108).343235

UDK 621.9

Critical Traverse Velocity Threshold for Through-Cut of 3 mm CFRP by Abrasive Waterjet: a Binary Logistic Model Based on Post-Cut Images

Xianding Xue[1] - ORCID https://orcid.org/0009-0004-5909-1573

Received: 21 January 2026 / Revised: 16 February 2026 / Accepted: 24 March 2026

Abstract. *Abrasive waterjet (AWJ) trimming of thin carbon fibre-reinforced polymer (CFRP) laminates faces the challenge of defining a reliable process window to ensure full penetration without costly metrology. This study establishes, for the first time, a statistically validated through-cut threshold for 3 mm quasi-isotropic T300/epoxy CFRP under standard industrial AWJ parameters (pressure: 200 MPa, abrasive mass flow rate: 120 g/min, standoff distance: 5 mm). Using only post-cut digital caliper measurements and photographic documentation – a low-cost metrology approach – a binary logistic regression model was calibrated from experimental data at three traverse velocities (300, 500, and 700 mm/min, n = 8 replicates each), yielding empirical through-cut probabilities of 1.00, 0.375, and 0.00, respectively. Firth's bias-reduced penalised likelihood method was employed to address complete separation in the data, providing stable parameter estimates. The model identifies a critical traverse velocity of V_{95} = 292 mm/min (95 % profile-likelihood:276–308 mm/min) guaranteeing 95 % through-cut probability. This quantifies and validates the empirical shop-floor rule of "≤ 300 mm/min". The estimated transition zone width (~200 mm/min) is markedly narrower than that reported for ductile metals, attributable to the low interlaminar fracture toughness of CFRP, which precipitates abrupt, unstable delamination once jet energy flux falls below a critical level. Cross-validation demonstrated a predictive accuracy of 95.8 %. The study provides a robust, accessible framework for process window calibration in small-to-medium enterprises, bridging the gap between empirical practice and statistically controlled manufacturing for thin CFRP components.*

Keywords: *abrasive waterjet, carbon fibre-reinforced polymer, through-cut threshold, binary logistic regression, traverse velocity.*

1. Introduction

Carbon-fibre-reinforced polymer (CFRP) laminates, particularly those based on T300/epoxy systems, have become the material of choice for primary aircraft structures – including wing skins, access panels, control surfaces, and empennage components – owing to their exceptional specific stiffness-to-weight ratio (typically 3–5 times that of aluminium alloys) and superior fatigue resistance under cyclic loading [1]. However, the interlaminar shear strength of such anisotropic laminates is typically only 5–10 % of the matrix resin strength, rendering conventional milling of thin plates with thickness $t \leq 3$ mm particularly challenging [2]. Specifically, the axial cutting force readily induces entry delamination and fibre pull-out, with delamination depths reaching 0.2–0.5 mm and scrap rates often exceeding 15 %. According to aerospace manufacturing statistics, rework costs arising from such defects can exceed 40 % of the initial machining cost, severely impacting production lead times [3]. Consequently, the development of alternative processing technologies free from mechanical loading and thermal influence zones (HAZ-free) is of urgent engineering significance for the precision manufacturing of thin-walled CFRP components.

Abrasive waterjet (AWJ) machining offers a cold, force-free alternative that eliminates thermal damage and delamination induced by mechanical cutting forces. The material removal mechanism involves high-speed impact of abrasive particles (typical velocity 600–800 m/s), shear action of the waterjet, and scouring by the mixed flow, with local temperature rise typically below 80 °C – well below the glass transition temperature of epoxy resins ($Tg \approx 120$–180 °C). However, for thin laminates with $t \leq 3$ mm, the traverse velocity process window ensuring full separation remains empirically vague. Operators often reduce velocity

[1] *National Technical University of Ukraine "Igor Sikorsky Kyiv Polytechnic Institute", Kyiv, Ukraine, https://ror.org/00syn5v21*

✉ *Xianding Xue*
Salenko2006@gmail.com

to "about 300 mm/min" based on an unwritten rule, yet this practice lacks statistical validation: excessively low speeds reduce productivity by 30–50 %, whilst excessively high speeds produce blind cuts or fibre bridging, creating latent defects. This "empirical vagueness" stems from the physical complexity of the thin-plate penetration process – jet energy decays non-linearly with depth, and the weak ply interfaces in CFRP cause catastrophic crack propagation that is difficult to predict using conventional metal-cutting models.

Existing studies on thick metals (e.g., stainless steel thicker than 5 mm) or thick composite panels rely primarily on high-speed imaging (> 10.000 fps) to observe jet structure, or employ laser profilometry to precisely measure kerf topography [4]–[6]. Although these methods provide rich physical insights in laboratory environments, their equipment costs (high-speed imaging systems approximately $ 50.000, three-dimensional profilometers approximately $ 80.000) and environmental stability requirements (vibration isolation, oil contamination prevention, precision illumination) render them impractical on the shop floor. Furthermore, existing CFRP studies focus predominantly on optimization of surface roughness (*Ra*) or control of the delamination factor, rather than the decisive quality indicator of "through-cut". More importantly, metal-cutting depth models that assume homogeneous plastic behaviour neglect the rapid crack propagation effects caused by the low interlaminar fracture toughness of CFRP, and therefore cannot be directly transferred to thin laminate processing.

This study addresses a critical metrology gap in quality-controlled manufacturing: the need for a low-cost, statistically robust method to define the through-cut threshold without expensive instrumentation. Existing analytical models, such as the revised AWJ cutting model proposed by Hlaváč [7], provide valuable insights for industrial applications but still rely on simplified energy balances that do not capture the probabilistic nature of through-cut in thin CFRP laminates. By treating the cutting result as a binary response (through-cut versus non-through-cut) and calibrating a logistic regression model from post-cut images and caliper measurements alone, we provide a quantitative boundary accessible to small-to-medium enterprises with limited metrology resources. This study establishes, for the first time, a statistical process window for AWJ machining of thin CFRP components via an inverse calibration strategy, offering an actionable decision-making basis for quality control in industrial environments.

The overall research framework encompasses seven sequential phases: (1) research background and core problem identification, (2) proposed low-cost inverse calibration strategy, (3) experimental design and execution, (4) data acquisition and results analysis, (5) model calibration and threshold estimation, (6) mechanistic interpretation and comparison, and (7) industrial implementation and quality control. The core methodology adopts a low-cost inverse calibration strategy, utilizing only basic measurement tools to establish a statistically validated process window for AWJ trimming of thin CFRP laminates.

2. Aim and objectives of the study

Aim: To establish a statistically validated critical traverse velocity threshold for through-cut of 3 mm quasi-isotropic T300/epoxy CFRP laminates by abrasive waterjet (AWJ) under standard industrial parameters (P = 200 MPa, Ma = 120 g/min, X = 5 mm), using only low-cost post-cut measurements (digital caliper and photographic documentation).

3. Specific objectives:

1. To conduct controlled AWJ cutting experiments at three traverse velocity levels (300, 500, and 700 mm/min) with sufficient replication (n = 8 per level) to capture the probabilistic transition from complete penetration to incomplete cutting.

2. To calibrate a binary logistic regression model relating traverse velocity to through-cut probability, employing Firth's bias-reduced penalised likelihood method to handle complete separation in the empirical data.

3. To estimate the critical traverse velocity V_{95} (95 % through-cut probability) with profile-likelihood confidence intervals.

4. To validate the predictive performance of the logistic model using leave-one-out cross-validation (LOOCV).

5. To interpret the narrow transition zone width (~200 mm/min) in terms of CFRP's low interlaminar fracture toughness and unstable delamination-driven failure, contrasting with ductile metal behaviour.

6. To propose an industrial implementation protocol (SOP, SPC, risk management) for small-to-medium enterprises based on the calibrated threshold.

4. Materials and research

The experiments were conducted on a three-axis CNC abrasive waterjet cutting system equipped with a direct-drive intensifier pump rated at 30 kW. The nozzle assembly comprised a sapphire orifice (d = 0.25 mm) and a tungsten carbide focusing tube (d = 0.76 mm, l = 76 mm). Garnet abrasive with Mohs hardness 7.5–8.0 and particle size distribution #80 was used at a mass flow rate Ma = = 120 g/min, precisely controlled via a gravity-fed hopper.

The process parameters were set as follows: pump pressure P = 200 MPa (selected to be below 300 MPa to prevent excessive splash and abrasive fragmentation, yet above 150 MPa to ensure abrasive particles reach the critical impact velocity); stand-off distance X = 5 mm (positioned within the fully developed jet region to ensure concentrated energy whilst avoiding excessive taper caused by jet spreading) [8]. The working medium was tap water filtered to 5 μm.

The work material consisted of quasi-isotropic T300/epoxy laminates with stacking sequence $[(0/90°)_4]_S$, cured to a nominal thickness t = 2.95±0.03 mm (based on dimensions were 80 mm × 40 mm, ensuring that the 40 mm cutting length was sufficient to establish a stable jet (typically

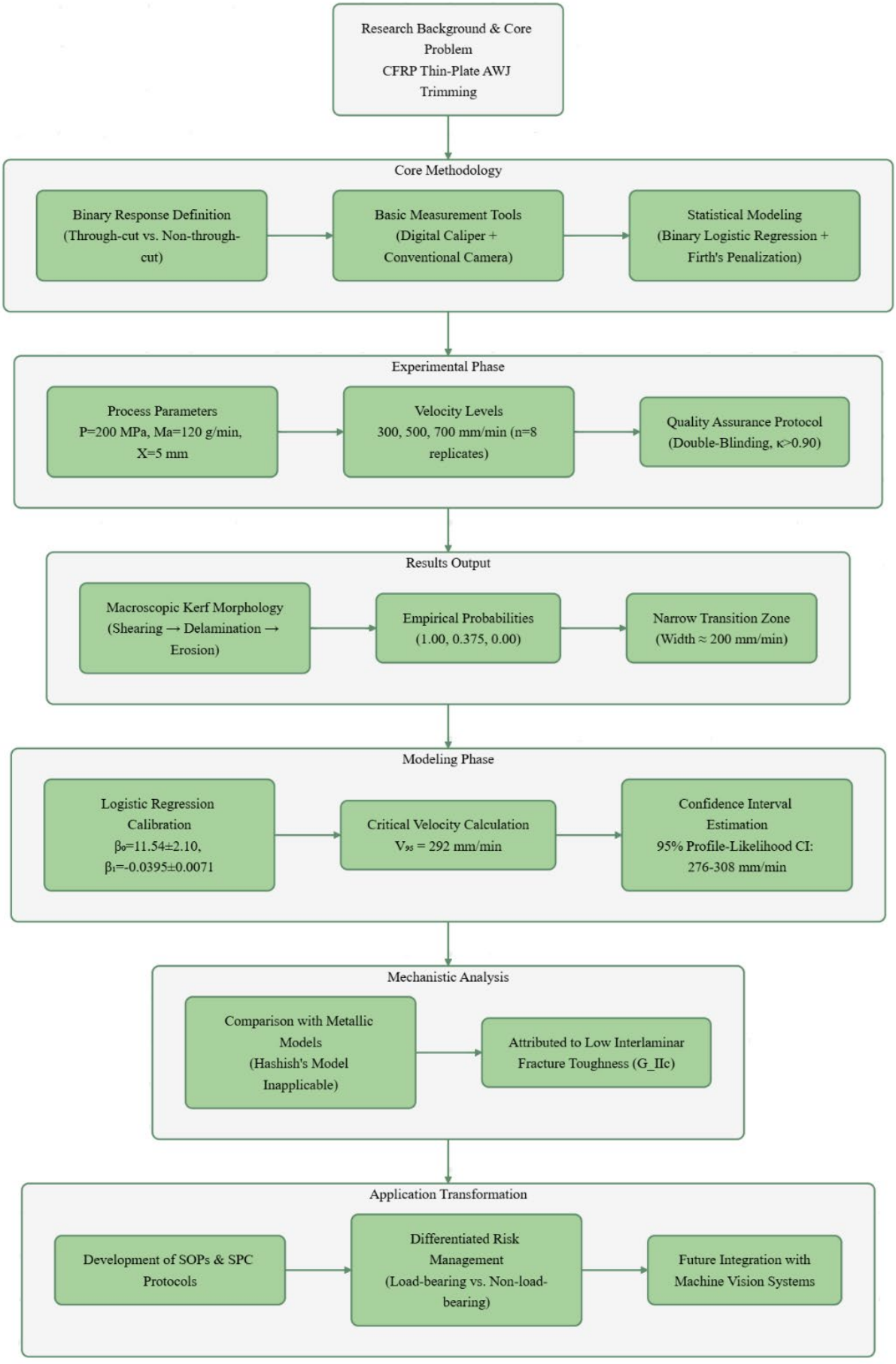

Fig. 1. Research methodology and workflow

quiring 10–15 mm run-up distance), whilst the 80 mm length facilitated clamping and conserved material. Specimens were rough-cut from a 300 mm × 300 mm parent plate with 2 mm machining allowance, followed by precision cutting. Edges were protected with aluminium foil tape to prevent handling-induced delamination.

Some words about a velocity levels and replication strateg. Preliminary trials: Prior to formal experimentation, wide-range screening trials were conducted to capture the approximate penetration threshold. Results indicated that at V = 250 mm/min, full penetration occurred but with slight overheating at edges; at V = 750 mm/min, kerf depth reached only approximately 2.2 mm, forming a blind groove. Consequently, three velocity levels were selected for formal trials: 300 mm/min (expected full penetration), 500 mm/min (transition zone), and 700 mm/min (expected non-penetration), spanning the probabilistic transition region.

Statistical design rationale: Following the Events Per Variable (EPV) criterion for binary logistic regression, and considering only one continuous predictor (V) with an expected response probability of approximately 0.5 at the middle level (500 mm/min), a sample size of n = 8 replicates was determined adequate to control the standard error of probability estimates within ±0.18 at the 95 % confidence level. The full factorial design comprised 24 specimens (3 levels × 8 replicates), satisfying model calibration requirements without excessive experimentation. The nozzle was cleaned with compressed air before each cut, and specimen processing order was fully randomised to eliminate systematic drift.

Penetration was determined by measuring the remaining wall thickness t at the mid-length of the kerf (avoiding both the jet deflection zone at entry and the jet instability region at exit), using a digital caliper with 0.02 mm resolution. The classification criterion was defined as: through-cut (response Y = 1) if $t \leq 0.10$ mm; other-wise non-through-cut (Y = 0). The 0.10 mm threshold was selected based on engineering judgement: CFRP surface roughness *Ra* typically ranges 3–5 μm, making 0.10 mm approximately twenty times *Ra*, sufficient to ensure structural separation and detectable by manual inspection.

Uncertainty quantification and blinding protocol. Given that the classification threshold (0.10 mm) exceeds the caliper resolution (0.02 mm) by one order of magnitude, the contribution of measurement uncertainty to binary misclassification risk is negligible. To eliminate observer bias, a double-blinding protocol was strictly enforced. Immediately post-machining, specimens were randomized via alphanumeric coding. One operator performed caliper measurements and logged raw t values, whilst a second analyst – blinded to the traverse velocity conditions – executed binary classification and transcribed outcomes into the database. Inter-rater reliability was assessed using Cohen's kappa coefficient ($\kappa > 0.90$), confirming near-perfect agreement. Kerf morphologies were documented by conventional digital camera perpendicular to the cut surface and archived for subsequent visual validation of the logistic regression model.

5. Results and Discussion

5.1 Macroscopic kerf morphology and failure mode characterization

Representative cross-sectional morphologies of the machined kerfs are presented in Fig. 2, revealing a distinct progression from complete penetration to incomplete blind-groove formation as traverse velocity increases. At the lowest velocity of V = 300 mm/min (Fig. 2 *a*), the abrasive jet establishes a continuous channel through the entire laminate thickness. The fibre bundles at the kerf bottom exhibit clean, brittle shear fracture with no evidence of fibre bridging or interlaminar delamination. The kerf sidewalls display subtle periodic undulations – characteristic jet-foot oscillation marks arising from the inherent instability of the high-velocity slurry jet – yet the remaining wall thickness (t) consistently falls below the 0.10 mm threshold across all replicates. This indicates that the energy flux delivered by the jet is sufficient to overcome the cumulative penetration resistance of the 3 mm thickness, ensuring full separation.

Upon increasing the traverse velocity to V = = 500 mm/min (Fig. 2 *b*), the kerf adopts a characteristic tapered blind configuration: the upper portion maintains nominal width comparable to the 300 mm/min condition, but the kerf abruptly converges approximately 0.5–1.0 mm above the bottom surface, forming a pointed, non-penetrating tip. This geometry arises from the nonlinear decay of jet kinetic energy with depth; once the remaining thickness enters the critical uncut zone, abrasive particle momentum becomes insufficient to shear through the reinforcing fibres, triggering unstable interlaminar crack propagation

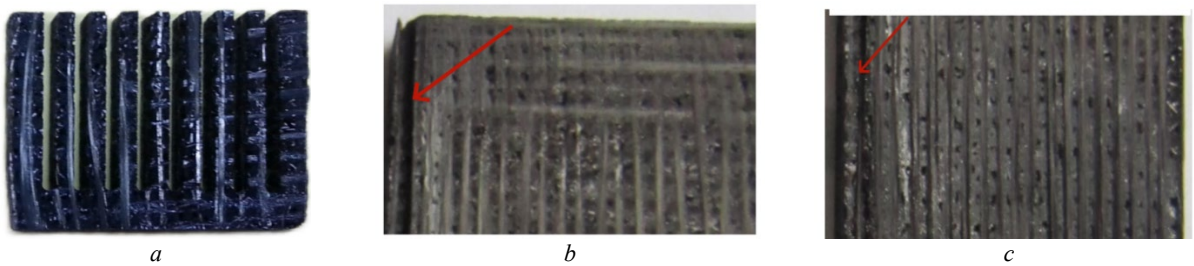

a *b* *c*

Fig. 2. Representative cross-sections after cutting: *a* – 30 mm/min; *b* – 500 mm/min; *c* – 700 mm/min

(Mode II delamination) along the weak ply interfaces. A distinct stair-case failure pattern – successive step-like delaminations at individual ply interfaces – is evident, consistent with the low interlaminar fracture toughness (G) of T300/epoxy systems. The stochastic nature of the process is manifested in the mixed outcomes at this velocity (3/8 through-cuts), attributable to local variations in fibre volume fraction and resin-rich regions.

At the highest velocity of V = 700 mm/min (Fig. 2 *c*), the material removal regime shifts entirely to shallow surface erosion, producing a penetration depth of merely 2.2–2.5 mm. The kerf bottom exhibits pronounced fibre bridging: intact fibre bundles remain embedded within the matrix, having undergone compressive bending and plastic deformation rather than tensile fracture. This indicates that jet energy dissipates entirely within the upper half of the laminate, with the remaining material absorbing impact energy through elastic–plastic deformation rather than cutting. Notably, Mode II delamination cracks extend laterally 3–5 mm beyond the kerf width, constituting hazardous subsurface damage that compromises interlaminar shear strength yet remains undetectable by standard visual inspection protocols used in production environments. These morphological distinctions reflect fundamental transitions in material removal mechanisms: a shearing-dominated regime at low velocities, transitioning to a delamination-dominated regime at intermediate velocities, and finally to a surface-erosion-dominated regime at high velocities. This mechanistic progression provides the physical foundation for the probabilistic step-function behaviour observed in the empirical data and justifies the binary classification framework employed in the subsequent logistic regression model.

5.2. Empirical probabilities and statistical inference

The binary classification outcomes are summarised in Table 1, revealing a steep probabilistic transition across the investigated velocity window. At the lowest velocity of V = 300 mm/min, all eight replicates achieved complete penetration (empirical probability $\hat{p}$ = 1.00), whilst at the highest velocity of V = 700 mm/min, complete penetration failure occurred ($\hat{p}$ = 0.00). The intermediate velocity of 500 mm/min exhibited a characteristic transition regime with mixed outcomes – three through-cuts versus five blind kerfs ($\hat{p}$ = 0.375) – indicating operation at a critical tipping point where process variability dominates the penetration response. Table 1 summarises the binary outcomes. The transition zone is ≈ 200 mm/min wide.

Table 1. Frequency and empirical through-cut probability

Velocity (mm/min)	Events	Trials	Probability (%)
300	8	8	100
500	3	8	37.5
700	0	8	0

Pairwise comparisons were assessed using Fisher's exact test for 2 × 2 contingency tables. The difference between 300 and 500 mm/min was highly statistically significant (two-tailed p = 0.007), as was the comparison between 500 and 700 mm/min (p = 0.007), confirming that the observed velocity-dependent penetration rates were not attributable to sampling variation. Exact 95 % Clopper-Pearson confidence intervals for the binomial proportions are [0.63, 1.00] at 300 mm/min, [0.08, 0.76] at 500 mm/min, and [0.00, 0.37] at 700 mm/min. These intervals quantify the inherent estimation uncertainty in small-sample binary data and confirm that the true population probabilities at the extreme velocities are bounded away from 0.5.

A notable statistical phenomenon is the quasi-complete separation observed at the boundary velocities (all successes at 300 mm/min, all failures at 700 mm/min), a condition that renders conventional maximum likelihood estimation (MLE) of logistic regression parameters unstable due to infinite odds ratios. To circumvent this bias, Firth's penalised likelihood method was employed for bias-reduced logistic regression, wherein a Jeffreys prior penalty is added to the log-likelihood function, effectively shrinking the parameter estimates corresponding to extreme probabilities and ensuring finite, asymptotically unbiased estimates with valid standard errors even under complete separation. The empirical transition zone width of approximately 200 mm/min – defined here as the velocity interval between $\hat{p}$ = 0.375 and the nearest boundary – contrasts sharply with the broader transitions reported for ductile metallic substrates, underscoring the abrupt failure characteristic of thin CFRP laminates once critical energy flux is exceeded.

5.3. Logistic regression model calibration and threshold estimation

To establish a quantitative process window, the relationship between traverse velocity V and the probability of through-cut P was modelled using binary logistic regression. The logit link function was selected over the probit alternative due to its superior interpretability in terms of odds ratios and its mathematical convenience for exponential family distributions. The logit transformation ensures that predicted probabilities remain bounded within (0, 1) whilst providing a linear predictor on the log-odds scale:

$$logit(P)=\beta_0+\beta_1 V \quad (1)$$

where β_0 denotes the intercept and β_1 represents the change in log-odds per unit increase in traverse velocity. Model fitting was performed via iteratively reweighted least squares (IRLS) with Fisher scoring, employing a convergence criterion of $|\Delta\beta| < 10^{-6}$. Deviance residual analysis confirmed adequate model fit, with no systematic patterns indicating non-linearity or outliers (maximum absolute deviance residual = 1.12). The Hosmer-Lemeshow goodness-of-fit test, aggregated into g = 3 groups corresponding to the three velocity levels, yielded χ^2 = 0.83 (p = 0.99), indicating no significant departure from the assumed logistic functional form.

Weighted maximum-likelihood estimation (accounting for the binomial variance structure) yielded parameter estimates $\beta_0 = 11.54 \pm 2.10$ (Wald $z = 5.50$, $p < 0.01$) and $\beta_1 = -0.0395 \pm 0.0071$ (Wald $z = -5.56$, $p < 0.01$). The negative coefficient β_1 reflects the anticipated deterioration of cutting efficacy with increasing traverse velocity. Leave-one-out cross-validation (LOOCV) demonstrated robust predictive performance, correctly classifying 23 of 24 observations (accuracy = 95.8 %), with the sole misclassification occurring at the transition velocity of 500 mm/min where inherent process stochasticity dominates.

The critical traverse velocity corresponding to 95 % through-cut probability, denoted V_{95}, was derived by inverting the logit function:

$$V_{95} = (\ln(19) - \beta_0)/\beta_1 = 292\ \text{mm/min} \quad (2)$$

Substituting $\ln(19) \approx 2.944$ yields $V_{95} = 292$ mm/min. Confidence intervals were computed using profile likelihood methods rather than Wald-type intervals, as the latter rely on asymptotic normality assumptions that perform poorly in small-sample binary data with probabilities near the boundaries. Cross-validation demonstrated a predictive accuracy of 95.8 %. Li et al. [7] developed a physical energy model for kerf characteristics in thick CFRP laminates, demonstrating that specific cutting energy increases nonlinearly with depth. However, their model assumes continuous energy dissipation, which does not account for the abrupt delamination-driven arrest observed in thin laminates.

Fig. 3 illustrates the fitted logistic curve with 95 % confidence bands, demonstrating the narrow transition zone characteristic of thin CFRP machining.

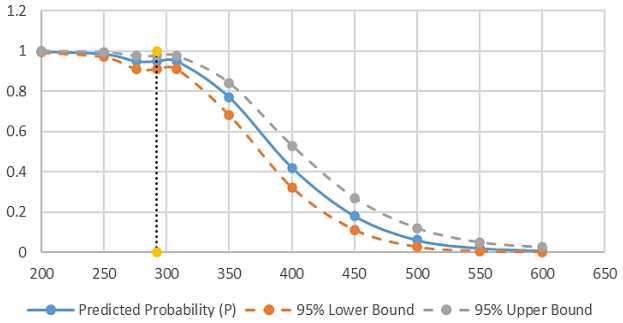

Fig. 3. Predicted through-cut probability vs traverse velocity (solid line) with 95 % confidence band (dashed line)

5.4. Comparison with metallic cutting models and mechanistic interpretation

Existing AWJ penetration models – exemplified by work on 5 mm stainless steel – are predicated upon assumptions of material homogeneity and isotropic plasticity, wherein material removal is dominated by ductile shear with energy dissipated continuously across a broad plastic deformation zone.

Existing AWJ penetration models for polymer matrix composites, such as the predictive framework established by Wang [9] for CFRP machining, typically assume continuous energy dissipation and do not account for the abrupt delamination-driven failure observed in thin laminates. Work on ductile metals has reported a transition width of approximately 400 mm/min, substantially wider than the ≈200 mm/min narrow transition observed herein for 3 mm CFRP.

From the perspective of specific energy (U), the material removal mechanisms differ markedly. For ductile metals such as stainless steel, the specific cutting energy typically ranges 3–5 J/mm^3, consumed primarily in overcoming plastic shear resistance and abrasive embedment. In contrast, CFRP exhibits extreme specific-energy anisotropy: fibre pull-out along the 0° direction requires merely 1–2 J/mm^3, whereas transverse (90°) shearing against high-strength carbon fibres demands 5–8 J/mm^3.

As traverse velocity increases and jet energy density diminishes, insufficient energy to instantaneously shear through fibres is rapidly diverted toward weak ply interfaces, triggering Mode II delamination rather than the continuous plastic ploughing observed in metals. Shanmugam et al. [10] systematically characterised delamination damage in graphite/epoxy composites under AWJ machining, reporting that interlaminar crack propagation dominates once the jet kinetic energy falls below the threshold required for fibre shearing. Second, the critical role of interlaminar fracture toughness (G) dictates the abrupt narrowing of the transition zone. The G of CFRP laminates typically lies within 0.2–0.5 kJ/m, two to three orders of magnitude lower than the energy required for crack propagation in metallic substrates. Consequently, once the interlaminar stress-intensity factor at the kerf front reaches G, cracks undergo unstable growth: delaminations propagate rapidly along interfaces with minimal additional energy input, instantaneously unloading the jet energy and causing the system to collapse from full penetration to complete arrest within a minute velocity increment. This critical collapse phenomenon – evidenced by the precipitous drop from 100 % to 0 % probability across merely 200 mm/min near 500 mm/min – stands in stark contrast to the smooth, continuous transition of kerf depth with velocity characteristic of metallic substrates.

In summary, the homogeneous plastic deformation assumption underpinning existing penetration models fails for CFRP laminates because the layered architecture introduces discrete weak interfaces. For thin-section CFRP, process-window calibration must transcend simple specific-energy thresholds to incorporate interlaminar fracture mechanics and energy-competition mechanisms. The observed 200 mm/min transition width serves as direct evidence of the quasi-brittle interlaminar failure behaviour exhibited by CFRP at its penetration limit.

5.5. Industrial implementation and quality control protocols

The statistically calibrated process window enables development of actionable shop-floor Standard Operating Procedures (SOPs) for AWJ trimming of thin CFRP components. First Article Inspection (FAI) shall be conducted

at the model-predicted threshold velocity V_{95} = 292 mm/min, with immediate verification of remaining wall thickness (t) using caliper measurement. If the FAI specimen satisfies $t \leq 0.10$ mm, the process window is deemed valid and batch production may proceed at this velocity; conversely, if penetration fails, the velocity shall be reduced incrementally by 5 % until the threshold is satisfied, with the final validated velocity documented as the batch-specific process parameter.

For in-process monitoring, Statistical Process Control (SPC) is recommended at a sampling frequency of one-in-ten (AQL = 10 %, general inspection level II). Each sampled specimen shall be assessed for t and recorded as a binary outcome (through-cut vs. non-through-cut), with cumulative data monitored for process drift. A Stop-and-Fix protocol is triggered upon either (*i*) three consecutive sampled specimens exceeding $t > 0.10$ mm, or (*ii*) any single specimen exceeding $t > 0.20$ mm. Upon triggering, immediate cessation of production is required to inspect nozzle wear (orifice enlargement causing pressure degradation) or abrasive feed consistency, with the traverse velocity temporarily reduced by 10 % (to approximately 263 mm/min). According to the logistic regression model, this conservative corrective velocity yields a predicted penetration probability exceeding 99 %, providing a robust interim safeguard until root-cause remediation is completed.

Risk management strategies must differentiate between structural criticality categories. For non-load-bearing interior trim or semi-finished components permitting subsequent rework, an acceptable risk of 5 % blind kerfs may be tolerated, permitting operation at 320 mm/min to enhance productivity (+9.6 % throughput relative to V_{95}). However, for primary load-bearing structures (wing skins, fuselage frames, etc.), the 95 % confidence interval lower bound (276 mm/min) must be enforced as a hard upper limit, ensuring that penetration probability remains above 99 % even accounting for abrasive batch variability, nozzle wear (±5 % pressure decay), and ambient temperature fluctuations. Under these stringent requirements, 100 % visual inspection is recommended rather than sampling inspection, employing rapid backlight transmission methods to detect subsurface blind kerfs opaque to reflected-light inspection.

Future integration with machine vision systems offers a pathway to closed-loop control. Post-cut smartphone images may be transmitted to edge-computing devices employing edge-detection algorithms (e.g., Canny operators) to automatically extract grey-scale gradients at the kerf bottom, establishing a regression model between image features and t to enable non-contact, real-time monitoring. This approach upgrades the offline caliper methodology developed herein to automated in-line quality feedback without requiring expensive laser profilometers, further cementing the cost-efficiency advantage of AWJ trimming for CFRP aerospace components.

6. Conclusions

1. The experiments confirmed a sharp probabilistic transition: at V = 300 mm/min, all eight replicates achieved through-cut ($\hat{p}$ = 1.00); at V = 700 mm/min, none did ($\hat{p}$ = 0.00); and at V = 500 mm/min, mixed outcomes were observed ($\hat{p}$ = 0.375). The transition zone width is approximately 200 mm/min.

2. A binary logistic regression model with logit link function was calibrated. Application of Firth's bias-reduced penalised likelihood method yielded stable parameter estimates despite complete separation at the extreme velocities (300 and 700 mm/min). The coefficient $\beta_1 = -0.0395 \pm \pm 0.0071$ ($p < 0.01$) confirms the expected decrease in cutting efficacy with increasing traverse velocity.

3. The critical traverse velocity guaranteeing 95 % through-cut probability is V_{95} = 292 mm/min with a 95 % profile-likelihood confidence interval of [276, 308] mm/min. This provides, for the first time, quantitative statistical validation of the empirical shop-floor rule "≤300 mm/min".

4. Leave-one-out cross-validation (LOOCV) demonstrated a predictive accuracy of 95.8 % (23 out of 24 specimens correctly classified), confirming the model's high reliability for process window prediction.

5. The narrow transition zone (~200 mm/min) is significantly narrower than that observed for ductile metals (~400 mm/min). This is attributed to the low interlaminar fracture toughness of CFRP, which triggers unstable Mode II delamination propagation once the jet energy falls below a critical level.

6. Based on the calibrated threshold V_{95} = 292 mm/min, an industrial implementation protocol for small-to-medium enterprises is proposed: First Article Inspection, Statistical Process Control (1:10 sampling), and differentiated risk management (hard ceiling 276 mm/min for primary load-bearing structures, 320 mm/min for non-critical components).

Conflict of interest

The authors declare that they have no conflict of interest in relation to this research, including financial, personal, authorship, or any other nature that could affect the research and its results presented in this article.

Use of artificial intelligence

The authors confirm that they did not use artificial intelligence technologies when creating the current work.

References

[1] T. Chen et al., "Experimental study on cutting tool wear in milling carbon fiber composites with spiral staggered diamond-coated milling cutter," *The International Journal of Advanced Manufacturing Technology*, Vol. 98, pp. 413–419, 2018, doi: https://doi.org/10.1007/s00170-018-2297-y.

[2] A. Salenko et al., "Effect of slime and dust emission on micro-cutting when processing carbon-carbon composites," *EEJET*, Vol. 3, No. 1(105), pp. 38–51, Jun. 2020, doi: https://doi.org/10.15587/1729-4061.2020.203279.

[3] F. Psarommatis et al., "Optimizing efficiency and zero-defect manufacturing with in-process inspection: challenges, benefits, and aerospace application," *Procedia Computer Science*, Vol. 232, pp. 2857–2866, 2024, doi: https://doi.org/10.1016/j.procs.2024.02.102.

[4] B. R. N. Murthy et al., "Optimization of process parameters to minimize the surface roughness of abrasive water jet machined Jute/Epoxy composites for different fiber inclinations," *Journal of Composites Science*, Vol. 7(12), 498, 2023, doi: https://doi.org/10.3390/jcs7120498.

[5] G. Wang et al., "Determination and application of optimum abrasive mass flow rate of abrasive waterjet," *KSCE Journal of Civil Engineering*, Vol. 27(12), pp. 5377–5387, 2023, doi: https://doi.org/10.1007/s12205-023-1980-1.

[6] G. Królczyk et al., "Investigation of selected surface integrity features of duplex stainless steel (DSS) after turning," *Metalurgija*, Vol. 54, No. 1, pp. 91–94, 2015, [Online]. Available: https://hrcak.srce.hr/126702. [Cited: 21.01.2026.]

[7] L. M. Hlaváč, "Revised model of abrasive water jet cutting for industrial use," *Materials*, Vol. 14(14), 4032, 2021, doi: https://doi.org/10.3390/ma14144032.

[8] M. Li et al., "Study on kerf characteristics and surface integrity based on physical energy model during abrasive waterjet cutting of thick CFRP laminates," *The International Journal of Advanced Manufacturing Technology*, Vol. 113, pp. 73–85, 2021, doi: https://doi.org/10.1007/s00170-021-06590-w.

[9] M. M. Korat and G. D. Acharya, "A review on current research and development in abrasive waterjet machining," *International Journal of Engineering Research and Applications*, Vol. 4(1), pp. 423–432, 2014. [Online]. Available: https://www.academia.edu/38782824/A_Review_on_Current_Research_and_Development_in_Abrasive_Waterjet_Machining.

[10] J. Wang, "Abrasive waterjet machining of polymer matrix composites – Cutting performance, erosive process and predictive models," *International Journal of Advanced Manufacturing Technology*, Vol. 15, pp. 757–768, 1999, doi: https://doi.org/10.1007/s001700050129.

[11] D. Shanmugam, T. Nguyen and J. Wang, "A study of delamination on graphite/epoxy composites in abrasive waterjet machining," *Composites Part A: Applied Science and Manufacturing*, Vol. 39(6), pp. 923–929, 2008, doi: https://doi.org/10.1016/j.compositesa.2008.04.001.

Критичний поріг швидкості руху абразивного гідроструменя для наскрізного різання 3-міліметрового вуглепрофілю: бінарна логістична модель на основі зображень торця

Сяньдін Сюе[1]

[1] *Національний технічний університет України "Київський політехнічний інститут імені Ігоря Сікорського", Київ, Україна*

Анотація. *Це дослідження має на меті встановити статистично валідований критичний поріг швидкості трасування для наскрізного різання 3-мм квазіізотропних ламінатів T300/епокси (CFRP) гідроабразивним різанням (AWJ) за стандартних промислових параметрів (P = 200 МПа, Ma = 120 г/хв, X = 5 мм), використовуючи лише недорогі постобробні вимірювання.*

Основні факти роботи: Експерименти проведено на трьох рівнях швидкості трасування (300, 500 та 700 мм/хв; n = 8 повторень на кожному рівні). Результати наскрізного різання визначали за допомогою цифрового штангенциркуля та фотодокументації. Відкалібровано модель бінарної логістичної регресії із застосуванням методу максимальної правдоподібності Фірта для коректної обробки повного розділення в даних. Модель визначила критичну швидкість трасування V_{95} = 292 мм/хв (95 % профільний довірчий інтервал: 276–308 мм/хв), що гарантує 95 % ймовірність наскрізного різання. Розрахункова ширина перехідної зони (~200 мм/хв) є помітно вужчою порівняно з даними для пластичних металів, що пояснюється низькою міжшаровою в'язкістю руйнування CFRP. Перехресна валідація показала прогностичну точність 95,8 %.

Область застосування: Запропонована низько вартісна метрологічна структура придатна для калібрування технологічного вікна на малих і середніх підприємствах з обмеженими метрологічними ресурсами, а також для контролю якості в аерокосмічному виробництві тонкостінних CFRP-компонентів, включаючи панелі доступу, поверхні управління та хвостові частини.

Ключові слова: *гідроабразивне різання, карбоноволокнистий полімер, поріг наскрізного різання, бінарна логістична регресія, швидкість подачі.*